An Assessment of Change in Vegetation Density to Estimate Landscape Vulnerability of Munnar and its Surroundings, Western Ghats, Kerala

B. K. Jayaprasad[1], R. Anilkumar[2], Vincent A Ferrer[3]

[1]Scientist-E, National Centre for Earth Science Studies, Ministry of Earth Sciences, Thiruvananthapuram, India

[2]KSCSTE Emeritus Scientist, Department of Geography, University College, Thiruvananthapuram, India

[3]Project Scientist- B, National Centre for Earth Science Studies, Ministry of Earth Sciences, Thiruvananthapuram, India

Abstract: ***Assessment of temporal changes in the vegetation density in an area is essential in land dynamic studies oriented towards the understanding of the vulnerability of the landscape concerned. The present investigation is attempted to understand the vulnerability of the landscape comprising a segment of an ecologically sensitive hotspot of the world, the Munnar and its surroundings, extending between 76°53' 57.53" and 77° 14'42.97" East longitudes and 10° 02' 5.08" to 10° 18' 51.08" North latitudes with an areal extent of 554.290 Sq.km. The analysis has been attempted by generating NDVI using remotely sensed data of the area for a period of about three decades. The study exposed that a significant deterioration has occurred to the vegetative cover of the study area, the Munnar and its surroundings, and which increased the vulnerability of the landscape under investigation.***

Keywords: Landscape dynamics, Landscape vulnerability, NDVI, Vegetation stress, Munnar

1. Introduction

The pressure exerted by mankind in the form of deforestation has imposed a highly non-renewable impact on the forest ecology. A proper understanding about the trajectories of deforestation and landscape dynamics is inevitable for a sustainable management of the forest ecosystem (Pattanaik et al., 2011) which determines the climate of that region**.** This is achieved by means of assessing the vegetation stress and their exposure to the external influences over a long period of time. Remote Sensing data in the form of vegetation indices by far has shown wide application in appraising the vegetation trends as a function of landscape susceptibility and vulnerability due to external influences. **(**Hicke et al., 2003; Huang et al., 2010a; Kennedy et al., 2010; Smith et al. 2014). Numerous such vegetation indices have been developed and applied for assessing the vegetation health and their stress depending on the environmental setup that drives the vegetation stress. Some of the indices to be named are Normalized Difference Vegetation Index (NDVI), Soil Adjusted Vegetation Index (SAVI) and Enhanced Vegetation Index (EVI), of which NDVI is the one applied universally for vegetation-related monitoring in various studies (Hielkema et al.,1986; Im et al., 2012b; Li et al., 2013; Yuan et al., 2014; Zhang et al., 2003; Ke et al., 2015). NDVI time series data products from various satellite missions like AVHRR and MODIS have been very successfully applied for measuring the forest cover depletion and their dynamics (Beck & Goetz, 2011; Beck et al., 2007; Piao et al., 2011). The rate of change of greenness and brownness which is a driving parameter of the health composition and productivity of the vegetation is very well explained using the NDVI. (Raynolds et al., 2012; Raynolds et al., 2006; Stow et al., 2004; Verbyla, 2008; Walker et al., 2012; Ranson et al., 2004; Smith at al., 2014). The present study has made a similar attempt on one of the highly ecologically sensitive areas of the earth, Western Ghats region of India. The NDVI maps were generated and compared to assess the changes in the vegetation types. The analysis helped to understand the status quo on the reality of the stress experienced in this ecologically sensitive region.

2. Objective

The major objective of the investigation was to assess temporal changes in the vegetation density to understand the landscape dynamics and the resultant landscape vulnerability in Munnar region in Kerala, a most fragile and ecologically sensitive zone in the Western Ghats, a hotspot on the surface of the earth, using remote sensing technology, for making suggestions for the mitigation of landscape vulnerability.

3. Study Area

The study area (fig.1) "Munnar and its surroundings" in the Kerala State extends between 76°53' 57.53" and 77° 14' 42.97" East longitudes and 10° 02' 5.08" to 10° 18' 51.08" North latitudes. Total area covered is 554.290 Sq.km. Munnar is the part of Western Ghats represents geomorphic features of immense importance with unique biophysical and ecological processes. It controls the mountain weather pattern. It is a part of hottest hotspots of biological diversity and having high geological, cultural and aesthetic values.

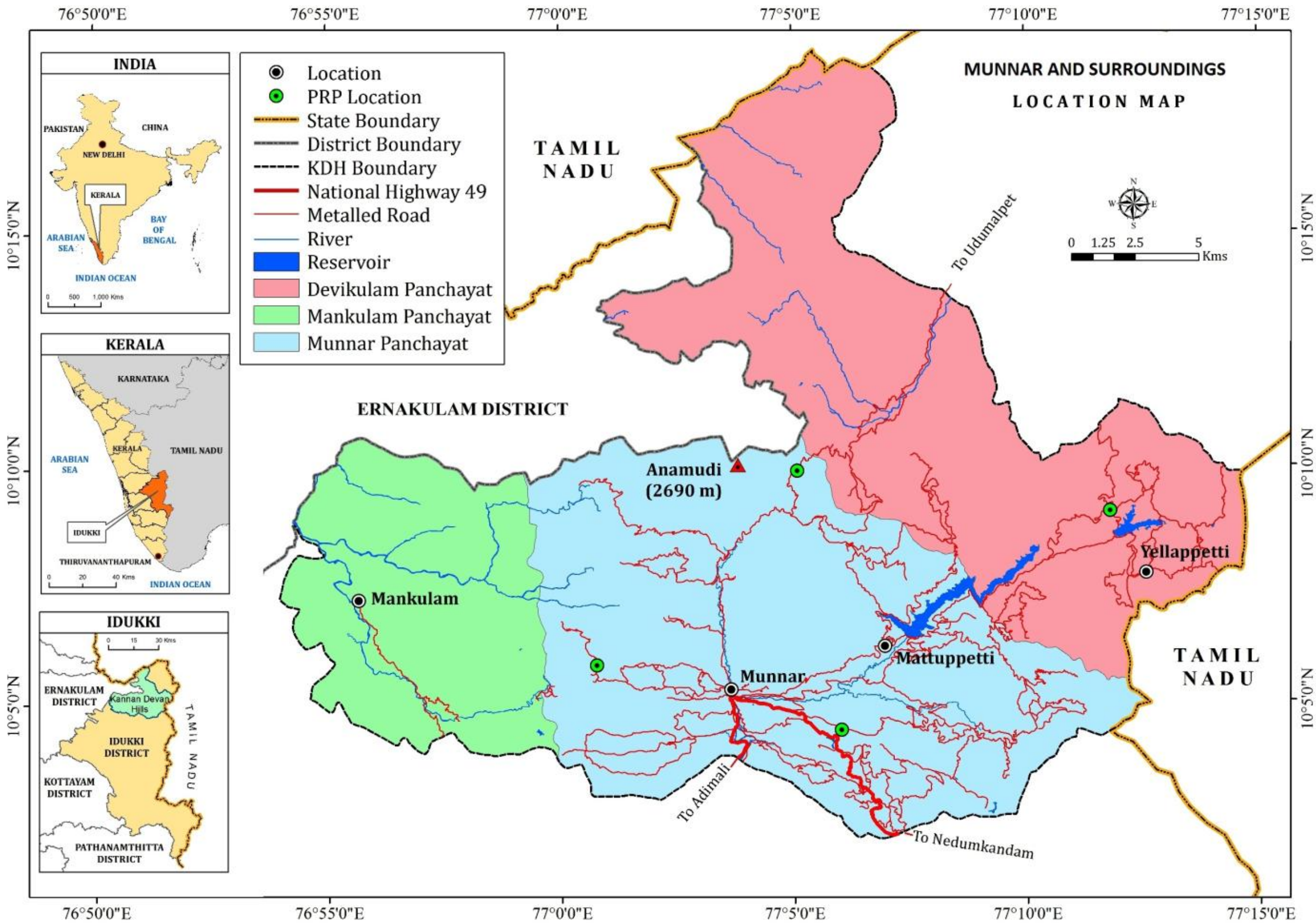

Figure 1: Study area

4. Database and Methodology

This study has used the Landsat data (Table-1) for the three periods to study the landscape changes that has occurred over the study area. The data products consist of the Thematic Mapper (TM) from the Landsat 5 satellite, the Enhanced Thematic Mapper (ETM+) from the Landsat 7 and the Operational Land Imager (OLI) from the Landsat 8 satellite .

Table 1

Sl. No.	*Satellite*	*Sensor*	*Date of Pass*	*Path/Row*	*Spatial Resolution (m)*	*Equatorial crossing time*
1	Landsat 5	TM	19-01-1988	144/053	30	9.45 am
2	Landsat 7	ETM+	18-02-2002	144/053	30	10.00 am
3	Landsat 8	OLI	16-01-2016	144/053	30	10.11 am

The satellite imageries were downloaded from the Earth explorer portal of USGS http://earthexplorer.usgs.gov/. The satellite imageries provided to the user with the pixel values representing the strength of the at sensor radiance were rescaled to the radiometric resolution as Digital Number (DN). Though it is alright to just work directly with the DN values which in a way more or less represent the same scenario, but it is not always satisfactory when multiple sensor data for multiple temporal periods are being used especially in change detection studies. This issue has been resolved by applying a radiometric calibration for the data products used in the study.

5. Radiometric Calibration

The capability of perceiving and enumerating the vagaries occurring on the Earth's surface and its environment is highly dependent on the sensors that collect and provide data through space and time. This as expected can vary depending on the time and environmental conditions prevail during data acquisition in addition to the sensor characteristics and hence the correct interpretation of the scientific information over a long-term temporal satellite data for a region demands the capability to differentiate the artefacts caused in the data products due to sensor as well as changes in the Earth processes that are being monitored. (Roy et al., 2002). Hence the radiometric characterization and calibration of the data becomes a prerequisite for generating more reliable data. The calculation of the at-sensor spectral radiance is the fundamental stage in radiometric calibration wherein the DN value is converted into the at-sensor spectral radiance (L_λ) by using the minimum and maximum rescaling factors used for generating the DN values.

For the Landsat 5 & 7 datasets used in this study, the conversion of DN to L_λ is given by

$$L_\lambda = \left(\frac{LMAX_\lambda - LMAX_\lambda}{Q_{calmax} - Q_{calmin}}\right)(Q_{cal-}Q_{calmin}) + LMIN_\lambda \quad (1)$$

Where
L_λ = Spectral radiance at the sensor's aperture [W/(m^2 sr µm)]
Q_{cal} = Quantized calibrated pixel value [DN]
Q_{calmin} = Minimum quantized calibrated pixel value corresponding to $LMIN_\lambda$ [DN]
Q_{calmax} = Maximum quantized calibrated pixel value corresponding to $LMAX_\lambda$ [DN] $LMIN_\lambda$ = Spectral at-sensor radiance that is scaled to Qcalmin [W/(m^2 sr µm)]
$LMAX_\lambda$ = Spectral at-sensor radiance that is scaled to Qcalmax [W/(m^2 sr µm)].

The second step involved the computation of the exo-atmospheric Top of the Atmosphere (TOA) reflectance. Computation of the TOA reflectance can be envisaged to possess three advantages. In addition to removing the cosine effect of the different solar zenith angles caused by the varying time of data acquisition, the conversion to TOA reflectance also compensated for the difference in solar irradiances arising from the different spectral bands and corrects for the varying earth – sun distance between different times of data acquisition. The conversion of L_λ to TOA reflectance (**ρ_λ**) is given by

$$\rho_\lambda = (\pi * L_\lambda * d * d)/(ESUN_\lambda * \cos\theta_s) \quad (2)$$

Where
ρ_λ = Planetary TOA reflectance [unitless]
π = Mathematical constant equal to ~3.14159 [unitless]
L_λ = Spectral radiance at the sensor's aperture [W/(m^2 sr µm)]
d = Earth–Sun distance [astronomical units]
$ESUN_\lambda$ = Mean exoatmospheric solar irradiance [W/(m^2 µm)]
θ_s = Solar zenith angle [degrees]

The parameters required for the above equations which are variables with respect to image acquisition can be used from the metadata of the particular data whereas the constants like the earth – sun distance and ESUN values are acquired from Chander et al., (2009).

In case of the Landsat 8 OLI, the various rescaling parameters required for conversion from the DN value to the at-sensor radiance (L_λ) is consolidated and provided as a single rescaling factor and hence L_λ for OLI is given as

$$L_\lambda = M_L Q_{cal} + A_L \quad (3)$$

where:
L_λ = TOA spectral radiance (Watts/(m2 * srad * µm))
M_L = Band-specific multiplicative rescaling factor
A_L = Band-specific additive rescaling factor
Q_{cal} = Quantized and calibrated standard product pixel values (DN)

The value of M_L and A_L are provided with the metadata of every product and it can be used for the processing of the data products.

The conversion of L_λ to the TOA reflectance not corrected for solar angle in case of OLI is given as

$$\rho_\lambda' = M_\rho Q_{cal} + A_\rho \quad (4)$$

where
ρ_λ' = TOA planetary reflectance without correction for solar angle.
M_ρ = Band-specific multiplicative rescaling factor
A_ρ = Band-specific additive rescaling factor
Q_{cal} = Quantized and calibrated standard product pixel values (DN)
The TOA reflectance (ρ_λ) corrected for the solar angle is given by

$$\rho_\lambda = \rho_\lambda' / \cos\theta_s \quad (5)$$

where
ρ_λ = TOA planetary reflectance
θ_s = Local solar zenith angle

Applying the above equations based on the rescaling values (Landsat 8 User Manual), the three Landsat datasets were processed to generate the TOA reflectance bands which are used to calculate the Normalised Difference Vegetation Index (NDVI).

NDVI Estimation
Any landscape dynamics study making use of vegetation basically considers the health of the vegetation and their density or lushness of that particular region. Any changes in this scenario is brought out mainly by the changes in the chlorophyll content and the intracellular spaces in the spongy mesophyll of plant leaves. This phenomenon is highlighted by NDVI which is the normalized difference between the near infrared (NIR) and visible red reflectance (Rouse, et al., 1974; Tucker, 1979) bands (Gao, 1996; Gu, et al., 2008). This can otherwise be defined as the greenness value of the particular pixel in the given data product which is given by

$$NDVI = (NIR[Band\ 4] - RED[Band\ 3])/(NIR[Band\ 4] + RED[Band\ 3]) \quad (6)$$

In case of Landsat 8 OLI, the band designations are fixed at NIR for band 5 and RED for band 4. Hence the NDVI is calculated accordingly. The calculated NDVI value ranges from -1 to +1 wherein any value less than 0 is defined as non-vegetation and any pixel value above 0 upto 1 will represent vegetation with different concentrations or greenness and density which can be graded accordingly from sparse vegetation, moderate vegetation, High vegetation and Dense vegetation (Aburas et al., 2015).

6. Results and Discussion

The vegetation greenness classification for the three periods viz., 1988, 2002 and 2016 were estimated by generating the NDVI raster layers and classified into five classes as discussed earlier (Fig. 2 to 4). The area under each class is calculated and the change in the area over the period of time for each class is estimated. The non-vegetation region comprises of the all the features other than vegetation which in the study area has been attributed to the settlements, water bodies and rocky exposures. Being composed mainly of tea estates, the settlements which are being very sparsely distributed could not be identified within a pixel range considering the spatial resolution of Landsat data. This in turn has led the water body to take most of the non-vegetation contribution along with the exposed rocky regions. The total region under non-vegetation is very low, even though compared to 1988; a slight increase in the total area under non-vegetation region is seen in 2002. The increase in the area observed in 2016 is due to expansion of settlements in the Munnar region as reported during field verification. The same scenario was found to occur in the case of sparse vegetation which marked an increase in total area during the period between 1988 and 2002 which has further decreased during the period between 2002 and 2016, but it recorded an overall increase from 1988. The moderate vegetation and the dense vegetation categories share the overall vegetation cover of the total study area. The prevalent vegetation types/categories of the region are tea and evergreen forest. It is observed that from 1988 the area under evergreen forest has been drastically reduced as a linear trend over the years. This drastic decrease in area was found as an additive component in the category of moderate vegetation. In terms of NDVI scenario, a shift from the high vegetation category to the moderate vegetation can be attributed to various reasons like reduction in vegetation, reduction in density or concentration and even relating to the health of the vegetation like browning of the leaves or any impact of temperature and lack of rainfall. Hence the evergreen forest being classified under dense vegetation in earlier periods has to reclassify due to, decrease in dense vegetation, can not to be interpreted as due to deforestation, as evident that the decrease has been computationally incremented into the moderate vegetation category. Yet it is assessed that the density of the evergreen forest is getting reduced over the period of time and thus changing the NDVI values in order to be classified into the lower classes. A further in depth observation into the dense vegetation class of 2016 has revealed that the fifth class, dense vegetation, has become highly insignificant. This has led to further examination of the scenario through the high resolution Google Earth imagery (figure – 5) of 2015 and 2003 which revealed that the greenness of the vegetation during 2016 has highly reduced compared to that of 2003.

This study has given a broad outline and a clear picture of the vegetation status of the study area based on which future studies are recommended in the direction as though there is no major threat to vegetation in terms of increase in settlements or population, the conversion of the evergreen forests into other cultivated regions or the decrease in the greenness which is a parameter of the measure of the health of the vegetation available in that region. Hence this study concludes that the major landscape vulnerability factors for the study area as evident from the analysis made using remote sensing technology are the change in crop type or vegetation types from forest to cultivation land and the stress of climate change on the health of the existing forest cover.

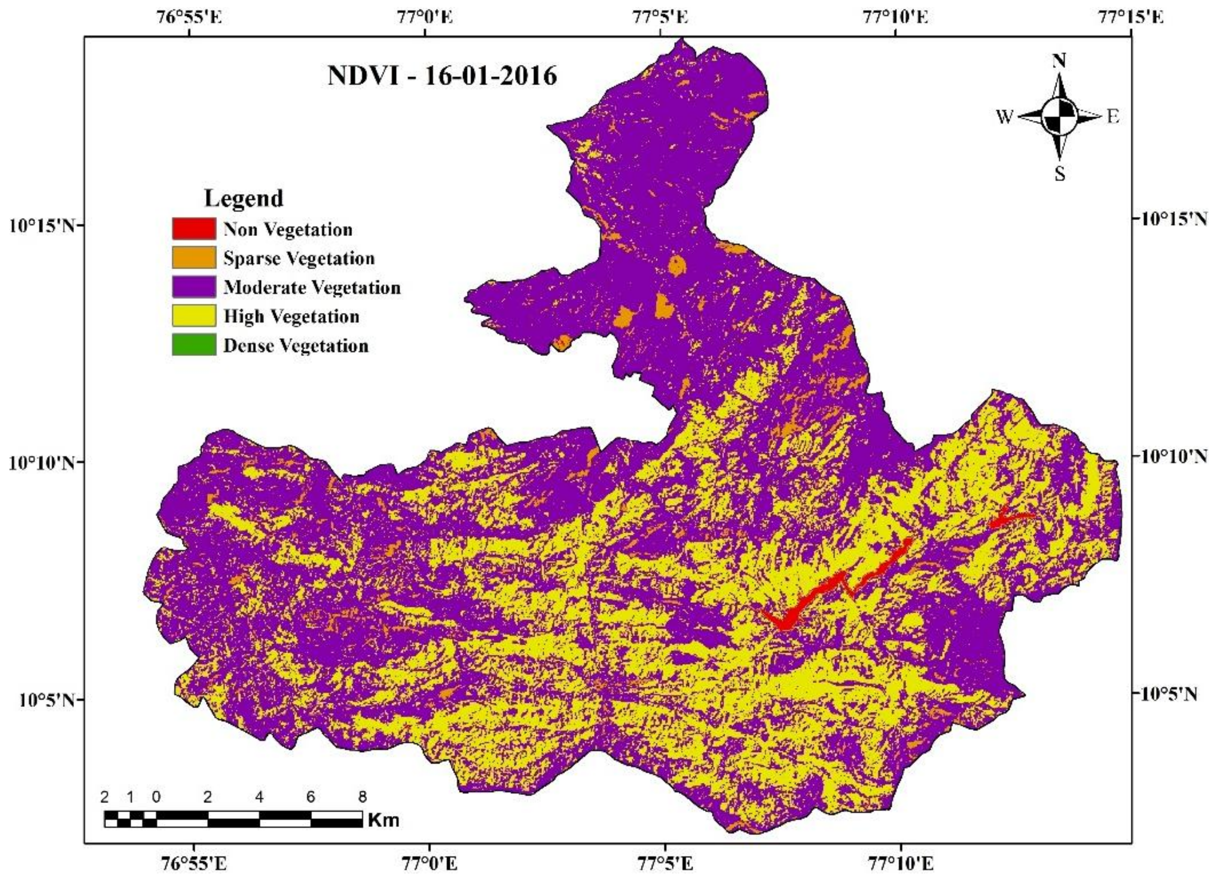

Figure 2

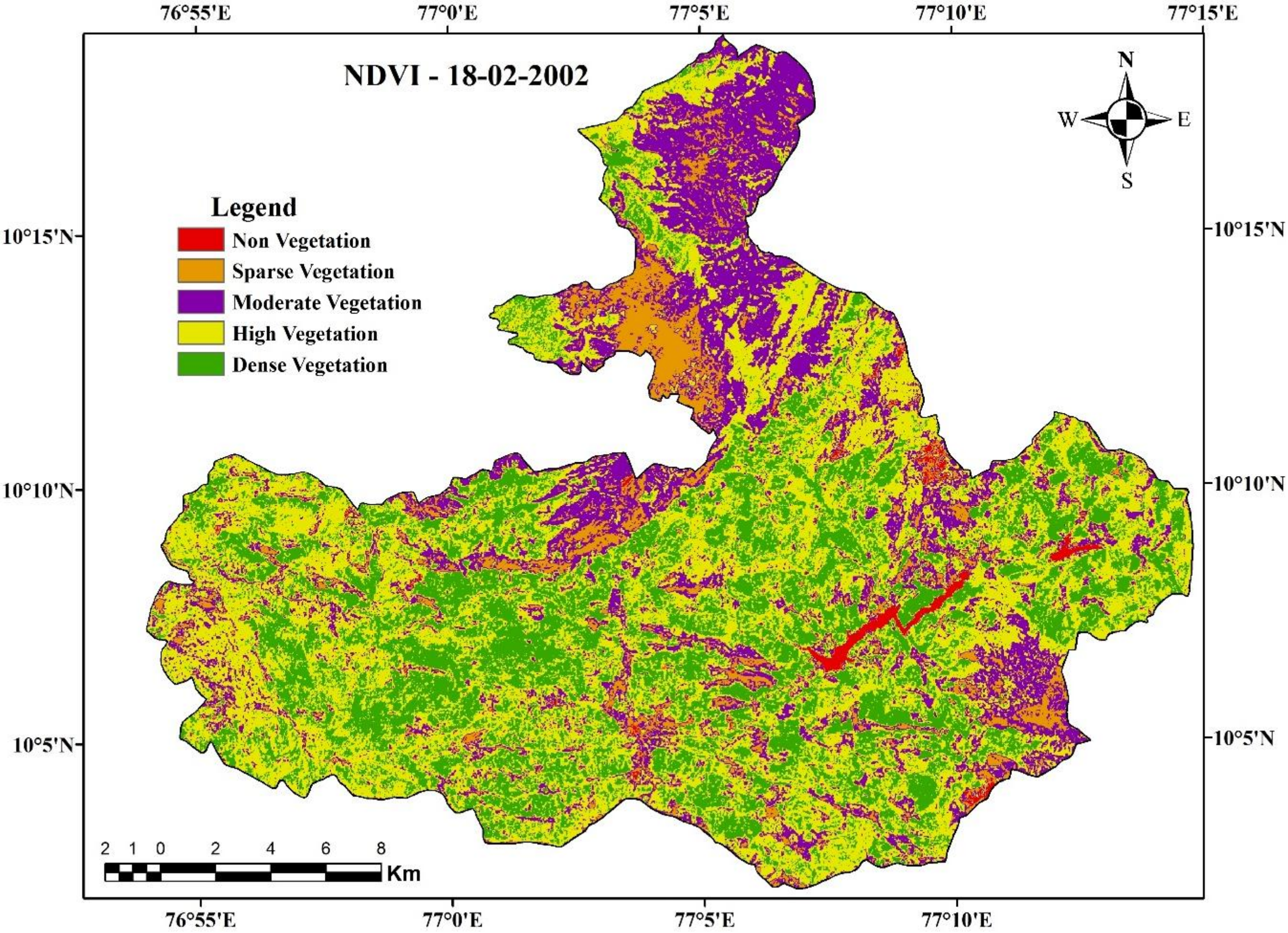

Figure 3

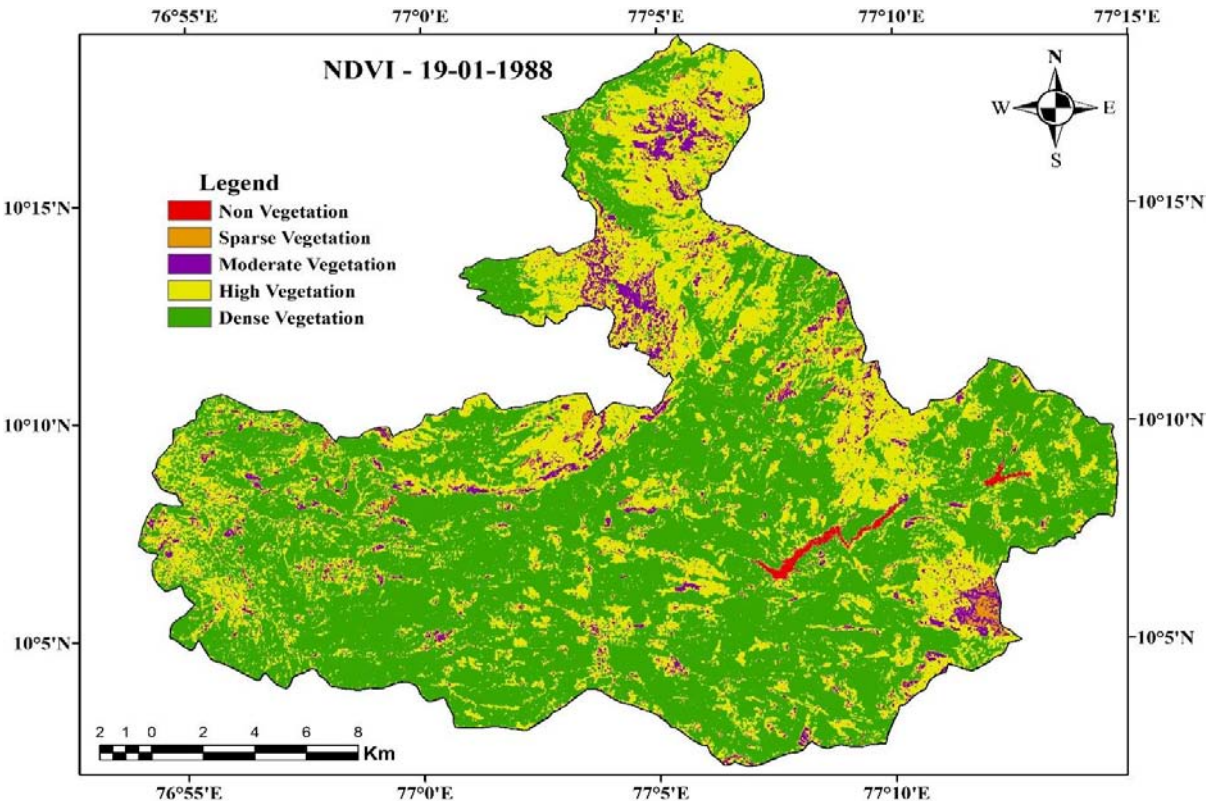

Figure 4

Figure 5: Vegetative cover 2015&2003

7. Acknowledgement

Authors are grateful to the Director, National Centre for Earth Science Studies, Thiruvananthapuram for extending facilities and encouragement to complete the investigation. Kerala State Committee on Science Technology and Environment is acknowledged for providing Emeritus Scientist Fellowship to the second author for continuing his research activities.

References

[1] Aburasa, M. M., Abdullaha, S. H., Ramlia, M. F., Ash'aari, Z. H. (2015). Measuring land cover change in Seremban, Malaysia using NDVI index. Procedia Environmental Sciences, 30, 238 – 243.

[2] Beck, P.S., Goetz, S. J. (2011). Satellite observations of high northern latitude vegetation productivity changes between 1982 and 2008: ecological variability and regional differences. Environmental Research Letters, 045501.

[3] Beck, P.S., Jonsson, P., Hogda, K. A., Karlsen, S. R., Eklundh, L., Skidmore, A. K. (2007). A ground-validated NDVI dataset for monitoring vegetation dynamics and mapping phenology in Fennoscandia and the Kola Peninsula. International Journal of Remote Sensing, 28, 4311–4330.

[4] Chander, G., Markham, B. L., Helder, D. L. (2009). Summary of current radiometric calibration coefficients for Landsat MSS, TM, ETM+, and EO-1 ALI sensors. Remote Sensing of Environment, 113, 893 – 903.

[5] Epstein, H. E., Raynolds, M. K., Walker, D. A., Bhatt, U. S., Pinzon, J. E. (2012). Dynamics of above ground phytomass of the circumpolar Arctic tundra during the past three decades. Environmental Research Letters, 7, 015506.

[6] Fuller, R. M., Groom, G. B., Jones, A. R. (1994). The land cover map of Great Britain: An automated classification of Landsat Thematic Mapper data. Photogrammetric Engineering and Remote Sensing, 60, 553−562.

[7] Gao, B. (1996). NDWI—A normalized difference water index for remote sensing of vegetation liquid water from space, Remote Sens. Environ., 58, 257–266.

[8] Goward, S., Irons, J., Franks, S., Arvidson, T., Williams, D., Faundeen, J. (2006). Historical record of Landsat global coverage: Mission operations, NSLRSDA, and international cooperator stations. Photogrammetric Engineering and Remote Sensing, 72, 1155−1169.

[9] Gu, Y., Hunt, E., Wardlow, B., Basara, J. B., Brown, J. F., Verdin, J. P. (2008). Evaluation of MODIS NDVI and NDWI for vegetation drought monitoring using Oklahoma Mesonet soil moisture data. Geophysical Research Letters, 35, L22401, doi:10.1029/2008GL035772.

[10] Hicke, J. A., Asner, G. P., Randerson, J. T., Tucker, C., Los, S., Birdsey, R., et al. (2003). Trends in North American net primary productivity derived from satellite observations, 1982–1998. Global Biogeochemical Cycles, 16(2), 1019. http://dx.doi.org/10.1029/2001GB001550.

[11] Hielkema, J.U., Prince, S.D., Astle, W.L. (1986). Rainfall and vegetation monitoring in the savanna zone of the Democratic Republic of Sudan using the NOAA Advanced Very High Resolution Radiometer. International Journal of Remote Sensing, 7(11), 1499–1513.

[12] Huang, C., Goward, S. N., Masek, J. G., Thomas, N., Zhu, Z., & Vogelmann, J. E. (2010a). An automated approach for reconstructing recent forest disturbance history using dense Landsat time series stacks. Remote Sensing of Environment, 114, 183–198.

[13] Im, J., Lu, Z., Rhee, J., Quackenbush, L.J. (2012b). Impervious surface quantification using a synthesis of artificial immune networks and decision/regression trees from multisensor data. Remote Sensing of Environment, 117, 102–113.

[14] Ke, Y., Im, J., Lee, J., Gong, H., Ryu, Y. (2015). Characteristics of Landsat 8 OLI derived NDVI by comparison with multiple satellite sensors and in-situ observations. Remote Sensing of Environment, 164, 298 – 393.

[15] Kennedy, R. E., Yang, Z., & Cohen, W. B. (2010). Detecting trends in forest disturbance and recovery

using yearly Landsat time series: 1. LandTrendr - Temporal segmentation algorithms. Remote Sensing of Environment, 114, 2897–2910.
[16] Landsat 8 (L8) Data Users Handbook, Version 1.0, June 2015.
[17] Li, M., Im, J., Beier, C. (2013). Machine learning approaches for forest classification and change analysis using multi-temporal Landsat TM images over Huntington Wildlife Forest. GIScience and Remote Sensing, 50, 361–384.
[18] Lin, D. H., Johnson, D. R., Andresen, C., Tweedie, C. E. (2012). High spatial resolution decade-time land cover change at multiple locations in the Beringian Arctic (1948-2000s). Environmental Research Letters, 7, 025502.
[19] Masek, J. G., Vermote, Huang, C., Wolfe, R., Cohen, W., Hall, F., Kutler, J., Nelson, P. (2008). North American forest disturbance mapped from a decadal Landsat record. Remote Sensing of Environment, 112, 2914−2926.
[20] Pattanaik, C., Reddy, S. C., Reddy, M. P. (2011). Assessment of spatial and temporal dynamics of tropical forest cover: A case study in Malkangiri district of Orissa, India. Journal of Geographical Sciences, 21(1), 176-192.
[21] Piao, S., Wang, X., Ciais, P., Zhu, B., Wang, T. A., Liu, J. I. (2011). Changes in satellite derived vegetation growth trend in temperate and boreal Eurasia from 1982 to 2006. Global Change Biology, 17, 3228–3239.
[22] Ranson, K. J., Sun, G., Kharuk, V. I., Kovacs, K. (2004). Assessing tundra-taiga boundary with multi-sensor satellite data. Remote Sensing of Environment, 93, 283–295.
[23] Raynolds, M. K., Walker, D. A., Epstein, H. E., Pinzon, J. E., Tucker, C. J. (2012). A new estimate of tundra-biome phytomass from trans-Arctic field data and AVHRR NDVI. Remote Sensing Letters, 3, 403–411.
[24] Raynolds, M. K., Walker, D. A., Maier, H. A. (2006). NDVI patterns and phytomass distribution in the circumpolar Arctic. Remote Sensing of Environment, 102, 271–281.
[25] Rouse, J. W., Jr., Haas, H. R., Deering, D. W., J. Schell, A., Harlan, J. C. (1974). Monitoring the vernal advancement and retrogradation (green wave effect) of natural vegetation. type III final report, 371 pp., NASA Goddard Space Flight Cent., Greenbelt, Md.
[26] Smith, A. M. S., Kolden, C. A., Tinkham, W. T., Talhelm, A. F., Marshall, J. D., Hudak, A. T., Boschetti, L., Falkowski, M. J., Greenberg, J. A., Anderson, J. W., Kliskey, A., Alessa, L., Keefe, R. F., Gosz, J. R. (2014). Remote sensing the vulnerability of vegetation in natural terrestrial ecosystems. Remote Sensing of Environment, 154, 322 – 337.
[27] Stow, D. A., Hope, H., McGuire, D., Verbyla, D., Gamon, J., Huemmrich, F., et al. (2004). Remote sensing of vegetation and land-cover change in Arctic tundra ecosystems. Remote Sensing of Environment, 89, 281–308.
[28] Townshend, J. R. G., Bell, V., Desch, A. C., Havlicek, C., Justice, C. O., Lawrence, W. E., Skole, D., Chomentowski, W. W., Moore, B., Salas, W., Tucjer, C. J. (1995). The NASA Landsat Pathfinder Humid Tropical Deforestation Project. Proceedings Land Satellite Information in the Next Decade, ASPRS Conference (pp. 76−87). Vienna, Virginia.
[29] Verbyla, D. (2008). The greening and browning of Alaska based on 1982–2003 satellite data. Global Ecology and Biogeography, 17, 547–555.
[30] Walker, D. A., Epstein, H. E., Raynolds, M. K., Kuss, P., Kopecky, M.A., Frost, G. V., et al. (2012). Environment, vegetation and greenness (NDVI) along the North America and Eurasia Arctic transects. Environmental Research Letters, 7, 015504.
[31] Wulder, M. A., White, J. C., Goward, S. N., Masek, J. G., Irons, J. R., Herold, M., Cohen, W. B., Loveland, T. R., Woodcock, C. E. (2008). Landsat continuity: Issues and opportunities for land cover monitoring. Remote Sensing of Environment, 112, 955−969.
[32] Yuan, F., Wang, C., Mitchell, M. (2014). Spatial patterns of land surface phenology relative to monthly climate variations: US Great Plains. GIScience and Remote Sensing, 51, 30–50.
[33] Zhang, X., Friedl, M.A., Schaaf, C.B., Strahler, A.H., Hodges, J.C., Gao, F., et al. (2003). Monitoring vegetation phenology using MODIS. Remote Sensing of Environment, 84(3), 471–475.